



American Society of Hematology
2021 L Street NW, Suite 900,
Washington, DC 20036
Phone: 202-776-0544 | Fax 202-776-0545
editorial@hematology.org

VEGF-C Protects the Integrity of Bone Marrow Perivascular Niche

Tracking no: BLD-2020-005699R1

Shentong Fang (Wihuri Research Institute, Finland) Shuo Chen (University of Helsinki, Finland) Harri Nurmi (Wihuri Research Institute, Finland) Veli-Matti Leppänen (Wihuri Research Institute, Finland) Michael Jeltsch (Wihuri Research Institute, Finland) David Scadden (Massachusetts General Hospital, Harvard Medical School, United States) Lev Silberstein (Fred Hutchinson Cancer Research Center, United States) Hanna Mikkola (University of California, Los Angeles, United States) Kari Alitalo (Wihuri Research Institute, Finland)

Abstract:

Hematopoietic stem cells (HSCs) reside in the bone marrow (BM) stem cell niche, which provides a vital source of HSC regulatory signals. Radiation and chemotherapy disrupt the HSC niche, including its sinusoidal vessels and perivascular cells, contributing to delayed hematopoietic recovery. Thus, identification of factors that can protect the HSC niche in an injury could offer a significant therapeutic opportunity to improve hematopoietic regeneration. Here we show a critical function for vascular endothelial growth factor C (VEGF-C) in maintaining the integrity of the BM perivascular niche and improving BM niche recovery after irradiation-induced injury. Both global and conditional deletion of *Vegfc* in endothelial or leptin receptor+ (LepR+) cells led to a disruption of the BM perivascular niche. Furthermore, deletion of *Vegfc* from the microenvironment delayed hematopoietic recovery after transplantation by decreasing endothelial proliferation and LepR+ cell regeneration. Exogenous administration of VEGF-C via adeno-associated viral vector improved hematopoietic recovery after irradiation by accelerating endothelial and LepR+ cell regeneration and by increasing the expression of hematopoietic regenerative factors. Our results suggest that preservation of the integrity of the perivascular niche via VEGF-C signalling may be exploited therapeutically to enhance hematopoietic regeneration.

Conflict of interest: No COI declared

COI notes:

Preprint server: No;

Author contributions and disclosures: F.S, S.C and H.N performed the experiments. V.L, M.J produced and provided VEGF-C protein. L.S. discussed the hypotheses; and contributed to data interpretation and manuscript writing. D.T.S. advised on experimental design and reviewed the manuscript. F.S, H.M and K.A conceived the project, designed experiments, analyzed and interpreted the data, and wrote the manuscript.

Non-author contributions and disclosures: No;

Agreement to Share Publication-Related Data and Data Sharing Statement: Data are available in the GEO database with accession number (GSE128464, GSE144420 and GSE153339). The data that support the findings of this study are available from the corresponding author upon reasonable request.

Clinical trial registration information (if any):

VEGF-C Protects the Integrity of Bone Marrow Perivascular Niche

Shentong Fang^{1,2}, Shuo Chen², Harri Nurmi^{1,2}, Veli-Matti Leppänen^{1,2}, Michael Jeltsch^{1,3,4},
David Scadden^{5,6}, Lev Silberstein⁷, Hanna Mikkola^{8*} and Kari Alitalo^{1,2*}

¹ Wihuri Research Institute, Haartmaninkatu 8, 00290 Helsinki, Finland

² Translational Cancer Medicine Program, Faculty of Medicine, Biomedicum Helsinki, University of Helsinki, 00014 Helsinki, Finland

³ Individualized Drug Therapy Research Program, Faculty of Medicine, University of Helsinki, Finland

⁴ Drug Research Program, Faculty of Pharmacy, University of Helsinki, Finland

⁵ Center for Regenerative Medicine, Massachusetts General Hospital, Boston, MA

⁶ Harvard Stem Cell Institute and Department of Stem Cell and Regenerative Biology, Harvard University, Cambridge, MA

⁷ Fred Hutchinson Cancer Research Center and University of Washington, Seattle, WA

⁸ Department of Molecular, Cell and Developmental Biology, Eli and Edythe Broad Stem Cell Research Center, University of California, Los Angeles, CA

Running title: *VEGF-C requirement for BM perivascular niche*

* Corresponding authors:

Hanna K.A. Mikkola

Department of Molecular, Cell and Developmental Biology

Eli and Edythe Broad Stem Cell Research Center

University of California, Los Angeles, CA

E-mail: hmikkola@mcdb.ucla.edu

and

Kari Alitalo,

Biomedicum Helsinki, PL63,

Haartmaninkatu 8, University of Helsinki,

FIN-00014 Helsinki, Finland, Tel: +358 2 941 25511

E-mail: kari.alitalo@helsinki.fi

Key points

- *Vegfc* deletion in endothelial or LepR⁺ cells compromises the bone marrow perivascular niche and hematopoietic stem cell maintenance.
- Exogenous administration of VEGF-C improves hematopoietic recovery after irradiation by accelerating endothelial and LepR⁺ cell regeneration.

Abstract

Hematopoietic stem cells (HSCs) reside in the bone marrow (BM) stem cell niche, which provides a vital source of HSC regulatory signals. Radiation and chemotherapy disrupt the HSC niche, including its sinusoidal vessels and perivascular cells, contributing to delayed hematopoietic recovery. Thus, identification of factors that can protect the HSC niche in an injury could offer a significant therapeutic opportunity to improve hematopoietic regeneration. Here we show a critical function for vascular endothelial growth factor C (VEGF-C) in maintaining the integrity of the BM perivascular niche and improving BM niche recovery after irradiation-induced injury. Both global and conditional deletion of *Vegfc* in endothelial or leptin receptor+ (LepR+) cells led to a disruption of the BM perivascular niche. Furthermore, deletion of *Vegfc* from the microenvironment delayed hematopoietic recovery after transplantation by decreasing endothelial proliferation and LepR+ cell regeneration. Exogenous administration of VEGF-C via adeno-associated viral vector improved hematopoietic recovery after irradiation by accelerating endothelial and LepR+ cell regeneration and by increasing the expression of hematopoietic regenerative factors. Our results suggest that preservation of the integrity of the perivascular niche via VEGF-C signalling may be exploited therapeutically to enhance hematopoietic regeneration.

Introduction

The BM niches for hematopoietic stem cells (HSC) are specialized multi-cellular units that control HSC quiescence and self-renewal¹⁻³. Perivascular HSC niche is composed of endothelial cells (ECs) and Leptin receptor+ (LepR+) stromal cells, which produce factors that regulate hematopoietic stem and progenitor cells (HSPCs) in a paracrine manner⁴⁻⁹.

Radiation and chemotherapy disrupt the BM perivascular niche, leading to regression and remodelling of ECs and adipogenesis of LepR+ cells¹⁰⁻¹⁵. HSC engraftment and proliferation after transplantation are supported by the BM microenvironment, including the perivascular niche^{10,13,16-19}. Thus, identification of factors that can protect the niche from irradiation damage or promote niche regeneration is of clinical interest, and may improve HSC transplantation efficacy. VEGF-VEGFR2 signalling is crucial for HSC maintenance and endothelial regeneration after transplantation, but not for LepR+ cell maintenance^{10,15,20}. A previous report showed that VEGF-C, another VEGF family member and a major lymphangiogenic factor, regulates fetal erythropoiesis²¹. VEGF-C is upregulated in BM ECs after sublethal irradiation²². We thus hypothesized that VEGF-C may be an important factor in the perivascular niche, especially during BM regeneration.

Here we show that VEGF-C maintains the LepR+ perivascular niche in the BM. Our results also revealed that loss of VEGF-C from the BM microenvironment delays vascular and hematopoietic recovery after transplantation. Viral vector mediated delivery of VEGF-C promoted the perivascular niche and hematopoietic recovery from irradiation-induced damage, suggesting that VEGF-C may have therapeutic potential.

Material and Methods

Mice and tissues. Animal experiments were approved by the Committee for Animal Experiments of the District of Southern Finland. The mouse lines *Vegfc*^{flox/flox}²³, *Rosa26-CreER*^{T2}²⁴, *Rosa26-LSL-tdTomato*²⁵, *Cdh5(BAC)-CreER*^{T2}²⁶, *Lepr-Cre*²⁷ have been described previously. All experiments were conducted in C57BL/6 genetic background. B6.SJL mice were purchased from The Jackson Laboratory. C57BL/6J (Envigo RMS B.V, UK) mice were used for AAV studies. Cre-mediated recombination in adult mice was achieved by administering five consecutive intragastric doses of tamoxifen (Sigma-Aldrich, MO, 20 mg/ml dissolved in 100 μ l corn oil) to *Vegfc*^{flox/flox}, *Rosa26-CreER*^{T2}; *Vegfc*^{flox/flox} (Cre+) and *Cdh5(BAC)-CreER*^{T2}; *Vegfc*^{flox/flox} (Cre+) mice. Adult C57bl/6J mice (8-10 weeks) received a single dose of a recombinant adeno associated virus serotype 9 (AAV9)-encoding mVEGFR3₁₋₄-Ig²⁸ (i.p., 10¹² virus particles in 200 μ l), AAV9 derived FL-mVEGFC²³ (i.p., 10¹¹ virus particles in 200 μ l) or VEGF-C protein²⁹. Control mice received AAVs that encoded domains four to seven of VEGFR3-Ig, only the Fc domain, or inactivated VEGF-C. Age and gender matched mice were used as controls.

Cell-surface Markers for Hematopoietic Stem and Progenitor cells. The following cell-surface markers were used: LKS (Lin-c-Kit+Sca1+), LT-HSC (FLT3-CD34-LKS or CD150+CD48-LKS), ST-HSC (FLT3-CD34+LKS), MMP (FLT3+CD34+LKS, or CD150-CD48-LKS), HPC-1 (CD150-CD48+LKS) and HPC-2 (CD150+CD48+LKS).

Flow Cytometry and Cell Sorting. Whole bone marrow (WBM) cells were obtained by flushing tibias and femurs with HBSS (Ca²⁺, Mg²⁺ free, Gibco™, Thermo Fisher Scientific, MA) supplemented with 2% fetal bovine serum (FBS). For niche cell analysis, mice were injected intravenously with 15 μ g of VE-Cadherin-Alexa-647 (BioLegend, CA) via tail vein 15 minutes prior to euthanasia. WBM was digested with Collagenase I (Worthington

Biochemical Corporation, NJ), Dispase II (Roche Applied Science, Switzerland) and DNase I (Sigma-Aldrich) in HBSS. Cells were resuspended in HBSS (Ca^{2+} , Mg^{2+} free) /2% FBS and stained using 1:200 dilutions of primary antibodies, unless otherwise indicated. Analysis and sorting were performed using FACS Aria II flow cytometer. Data were analysed using FlowJo v10 software (Tree Star Inc., OR).

scRNA-seq. Isolated CD45-Ter119-LepR-tdTomato+ cells and CD45-Ter119-VE-Cadherin+ cells from *Lepr-Cre;tdTomato* BM were resuspended in 0,04% bovine serum albumin and HBSS; and analysed using the Chromium Single-Cell 3'RNA-sequencing system (10x Genomics, Pleasanton, CA) with the Reagent Kit v2. Sample libraries were sequenced on Illumina NovaSeq 6000 system using S1 flow cell (Illumina, CA) with following read lengths: 26bp (Read 1), 8bp (i7 Index), 0 bp (i5 Index) and 91bp (Read 2).

CD45-Ter119-LepR+ cells and CD45-Ter119-VE-Cadherin+ cells purified from WT, $Vc^{i\Delta EC}$ and $Vc^{fl/fl}$ BM using LepR and VE-Cadherin antibodies, and lineage-CD45-Ter119- BM niche cells isolated from irradiated/non-irradiated $Vc^{i\Delta R26}$ and $Vc^{fl/fl}$ mice were analysed using the Chromium Single-Cell 3' Reagent Kit v3.1. Sample libraries were sequenced on Illumina NovaSeq 6000 system using S1 flow cell (Illumina, CA) with following read lengths: 28bp (Read 1), 8bp (i7 Index), 0 bp (i5 Index) and 89bp (Read 2).

Real-time quantitative PCR (qRT-PCR). Total RNA was isolated using the NucleoSpin® RNA II Kit (Macherey-Nagel, Germany) or RNeasy Micro Kit (QIAGEN, Germany). Q-PCR was carried out using either TaqMan Gene Expression Assays (Applied Biosystems, Thermo Fisher Scientific) accompanied with iQTM Supermix kit (Bio-Rad) or SYBR Green oligos with iQTM SYBR Green Supermix kit (Bio-Rad) on a Bio-Rad C1000 Thermal cycler.

Mouse Bone Marrow Transplantation. Recipient mice were lethally-irradiated 18 hours prior to transplantation with 10 Gy total body irradiation (split doses 2.5 hours apart) using gamma irradiator OB29/4 (STS, Braunschweig, Germany).

Bone sectioning, immunofluorescence and confocal microscopy. Freshly dissected femurs were fixed in 4% paraformaldehyde overnight at 4 °C. 100µm sections from the decalcified femurs were blocked in PBS containing 0.3% triton-X, 0.2% bovine serum albumin, 0.05% sodium azide and 5% normal donkey serum for 1h and stained with primary antibodies for two days, followed by incubation with secondary antibodies. Immunofluorescence images were taken with a Zeiss LSM780 confocal microscope (20X NA:0.80), or Zeiss Axioinvert microscope (5x NA:0.15;10x NA:0.3) (Carl Zeiss AG, Germany). Bright-field sections were viewed with a Leica DM LB microscope (Leica Microsystems, Germany) and images were captured with an Olympus DP50 color camera (Olympus Soft Imaging Solutions GmbH, Germany).

Statistical Analysis. All bar graphs represent mean \pm SD. All data is derived from two to four individual experiments. For comparisons of two experimental groups, two-tailed student's t-test was used (Graphpad Prism 8.0). For multiple comparisons, one-way ANOVA (Turkey's multiple comparisons test) was used (Graphpad Prism 8.0).

Detailed protocols are provided in the Detailed Experimental Procedures.

Results

VEGF-C is expressed in LepR+ cells and EC subsets in the BM

VEGF-C expression has been reported in hematopoietic cells and ECs in the developing embryo^{21,30}, and in adult smooth muscle³¹ and osteolineage cells³². To define the cell types in the adult mouse BM that produce VEGF-C, we first analyzed *Vegfc* mRNA level in BM cells by using quantitative PCR. We found that *Vegfc* expression was higher in non-hematopoietic LepR+ cells and PECAM1+ cells than in whole BM (WBM, Fig. 1A). We then performed single-cell RNA sequencing (scRNA-Seq) on LepR-tdTomato+ cells and VE-Cadherin+ ECs isolated from the BM of *Lepr-Cre;tdTomato* mice (Fig. 1B). Graph-based clustering was performed for about 6000 single-cell transcriptomes and visualized using uniform manifold approximation and projection (UMAP) (Fig. 1C). These clusters were: 1) two arterial EC (AEC) subsets (*Ly6a* arteriolar EC cluster; *Ly6a/Cd34* arterial EC cluster); 2) two sinusoidal EC clusters (*Stab-2* SECs-1 cluster; *Stab2/Klf4^{hi}* SECs-2 cluster); 3) five LepR subsets (*Lpl^{hi}* LepR-1 cluster; *Wisp2^{hi}* LepR-2 cluster; *Cxcl14^{hi}* LepR-3 cluster; osteo-lineage primed LepR-4 cells expressing *Wif1* and *Bgalp2*; fibroblast lineage LepR-5 cells expressing *Aspn* and *Col3a1* (Fig. 1C; Supplementary Figure 1 A). Cell projection using singleR³³ and three different published BM niche scRNA datasets³⁴⁻³⁶ as references confirmed these cell identities in our Seurat^{37,38} analysis (Supplementary Figure 1B-G). LepR-expressing cells, AECs, and some chondrocytes, SECs and fibroblasts expressed VEGF-C, as shown in our dataset and the three published reference-datasets³⁴⁻³⁶ (Fig. 1D; Supplementary Figure 1B-D). Two of the main receptors for VEGF-C, VEGFR-3 (*Flt4*) and VEGFR-2 (*Kdr*), were expressed in the ECs (Fig. 1D). Thus, both VEGF-C and its receptors are expressed in the adult BM perivascular niche.

VEGF-C regulates the integrity of BM LepR+ perivascular niche

To understand the functional significance of VEGF-C signalling on BM perivascular niche and hematopoiesis, we deleted *Vegfc* from 7-10-week-old *Vegfc* conditional knockout mice using the tamoxifen inducible *Rosa26-CreER^{T2}* recombinase ($Vc^{i\Delta R26}$) (Fig. 1E; Supplementary Figure 2A). By 7-months of age, immunofluorescence revealed a significantly smaller LepR+ BM area in $Vc^{i\Delta R26}$ mice than $Vc^{fl/fl}$ mice, whereas the endomucin+ vessel area was not significantly altered (Fig. 1F). Flow cytometry confirmed the decrease of LepR+ cells in relation to the PECAM1 stained ECs, which were not altered (Supplementary Figure 2B-C). A decrease of BM LepR+ cells in the absence of VEGF-C was recapitulated in wildtype (WT) mice in which VEGF-C was inactivated by “VEGF-C trap” involving AAV delivery of soluble mVEGFR-3₁₋₄-Ig²⁸ (Supplementary Figure 2J). These data suggested that VEGF-C is important for regulating the composition of the perivascular niche by maintaining the LepR+ cells.

Assessment of hematopoietic parameters revealed that the $Vc^{i\Delta R26}$ mice at 7-months of age had normal BM cellularity, spleen size, white blood cell (WBC) counts, BM lineage composition, and HSPC subtypes when analysed using the SLAM surface markers (CD48 and CD150, Fig. 1G; Supplementary Figure 2D-F). Similar results were obtained in analysis of HSPC numbers using CD34 and FLT3 as alternative surface markers (Supplementary Figure 2G-I). However, by 22-23-months of age, the $Vc^{i\Delta R26}$ mice had developed mild leukopenia and a significant reduction of HSCs and methylcellulose colony forming cells, despite their relatively intact BM cellularity and lineage composition (Fig. 1G; Supplementary Figure 2K-O). These data suggested that a prolonged disruption of the

perivascular niche due to VEGF-C loss compromises the long-term maintenance of normal hematopoiesis.

VEGF-C from a subset of ECs contributes to BM LepR+ cell maintenance

Since the scRNA analysis indicated that both BM LepR+ cells and ECs are sources of VEGF-C in the adult BM microenvironment, we crossed *Vegfc^{fl/fl}* mice with the corresponding cell type specific deleter mice. To evaluate whether ECs provide a functionally significant source of VEGF-C that supports the BM perivascular niche, we conditionally deleted *Vegfc* from adult BM ECs in *Cdh5(BAC)-CreER^{T2};Vegfc^{fl/fl}* (*Vc^{ΔEC}*) mice. Immunostaining for LepR and endomucin in femur sections and flow cytometry of LepR+ cells documented a significant decrease of LepR+ cells also in *Vc^{ΔEC}* mice, whereas the ECs were not significantly altered (Fig. 2A-B; Supplementary Figure 3A-B). Deletion of endothelial *Vegfc* resulted in a small but significant decrease of BM HSCs, whereas BM cellularity, spleen size, WBC counts, and BM lineage composition were not significantly altered (Fig. 2C; Supplementary Figure 3C-F).

VEGFR-2 and VEGFR-3 were expressed in BM ECs but not in LepR+ cells (Fig. 1D), suggesting that VEGF-C from ECs may indirectly regulate LepR+ cells in the perivascular niche. Although we did not observe significant phenotypic changes in the ECs, we suspected that signaling in ECs is altered after *Vegfc* deletion, and may be responsible for the loss of LepR+ cells in the *Vc^{ΔEC}* mice. Thus, we performed scRNA analysis of BM ECs and LepR+ cells isolated from *Vc^{fl/fl}* and *Vc^{ΔEC}* mice using flow cytometry (Fig. 2D-E; Supplementary Figure 4A,C). There were no significant changes in the percentages of BM SECs-1,-2, arteriolar or arterial ECs in these mice when analysed in Seurat-annotated EC subclusters (Supplementary Figure 4B). Nevertheless, analysis of differentially expressed

genes in endothelial clusters between $Vc^{i\Delta EC}$ mice and $Vc^{fl/fl}$ mice indicated that the expression of cell cycle inhibitor (*Cdkn1a*) and inflammation-related genes was upregulated in ECs from $Vc^{i\Delta EC}$ mice, whereas the hematopoietic niche factor *Cxcl12*⁵⁻⁸ was downregulated (Fig 2F; Supplementary Figure 4D). We confirmed the decrease of *Cxcl12* in the *Vegfc*-deleted ECs by q-PCR analysis (Fig. 2G). Functional annotation clustering analysis using the Database for Annotation, Visualization and Integrated Discovery (DAVID)^{39,40} and gene set enrichment analysis (GSEA) revealed that the biological processes associated with the genes up-regulated in endothelial subclusters from $Vc^{i\Delta EC}$ mice in comparison to $Vc^{fl/fl}$ mice were related to cellular response to interferon signalling and immune system response, whereas the down-regulated genes were associated with triglyceride and cholesterol homeostasis (Supplementary Figure 4E-G). This finding was consistent with the report showing that VEGF-C mediated stimulation of VEGFR-3 in LECs leads to down-regulation of genes involved in interferon responses⁴¹.

In addition to the reduced LepR+ cellularity, the scRNA-seq showed specific reduction of cells in LepR-2 and LepR-3 clusters in $Vc^{i\Delta EC}$ mice; these represent LepR+ cells closely related to SECs³⁴ (Fig. 2H). Differential gene expression analysis of the LepR+ cells in the scRNA-seq data indicated that *Pten* was decreased in LepR+ cells, which was confirmed by q-PCR analysis on isolated LepR+ cells (Fig. 2I-J; Supplementary Figure 4H-I). *Pten* has been shown to regulate the maintenance of LepR+ cells⁴². The decreased *Pten* level in LepR+ cells may thus contribute to the decrease of LepR+ cells in the BM. Niche factors *Vcam1*, *Angpt1* and *Csf1* were also decreased in LepR+ cells from $Vc^{i\Delta EC}$ mice, whereas some inflammation-related chemokine genes, for example *Cxcl9* and *Cxcl10*, were upregulated (Fig. 2I; Supplementary Figure 4H).

These data indicate that loss of VEGF-C from the ECs significantly impairs the expression of critical HSC-supporting genes in ECs and LepR⁺ cells. VEGF-C produced by ECs thus contributes to the normal endothelial program that supports LepR⁺ cells and HSCs.

VEGF-C from LepR⁺ cells contributes to BM vascular development and perivascular niche maintenance

To investigate if LepR⁺ cell-derived VEGF-C also contributes to perivascular niche integrity, we deleted *Vegfc* from LepR⁺ cells using the *Lepr-Cre* ($Vc^{\Delta Lepr}$) allele, which becomes active right after birth⁴². A decrease of the BM LepR⁺ areas as well as diaphyseal endomucin⁺ ECs was observed in femur sections of seven week old $Vc^{\Delta Lepr}$ mice. This result was consistent with reduction of VE-Cadherin and LepR expressing cells observed in flow cytometry analysis (Fig. 3A-B; Supplementary Figure 5A-B). The proliferation of ECs was decreased already in four week old $Vc^{\Delta Lepr}$ mice, which may explain a stronger vascular defect in these mice (Supplementary Figure 5C) than in mice in which *Vegfc* was deleted in adulthood (Figs. 1, 2). This suggests that the early loss of VEGF-C from the LepR⁺ cells compromises not only LepR⁺ cells in the perivascular niche, but also vascular development.

The $Vc^{\Delta Lepr}$ mice showed decreased HSC numbers and reduced methylcellulose colony forming ability at seven weeks of age (Fig.3C; Supplementary Figure 5E), whereas the BM cellularity, spleen size, WBC counts, and BM lineage composition were not significantly altered at this age (Supplementary Figure 5D-G). When $Vc^{\Delta Lepr}$ BM was transplanted competitively into lethally irradiated WT recipients, significantly impaired long-

term multilineage reconstitution was observed in all peripheral blood lineages between 8 and 16 weeks after transplantation (Fig. 3D). Mice transplanted with $Vc^{\Delta LepR}$ BM also showed a reduction in donor-derived LKS cells in the BM at 16 weeks after transplantation (Fig. 3E). Furthermore, we observed a reduced colony forming ability in CD150+CD48-HSCs from $Vc^{\Delta LepR}$ mice in primary methylcellulose cultures (Supplementary Figure 5H), indicating their compromised functional properties. As with endothelial-specific *Vegfc* deletion, a decrease in *Pten* level was also observed in LepR+ cells from the $Vc^{\Delta LepR}$ mice (Supplementary Figure 5I). These data suggest that VEGF-C produced by LepR+ cells is essential for BM vascular development, maintenance of LepR+ cells in the perivascular niche and for maintenance of a functional HSC pool.

Loss of VEGF-C from BM stroma delays vascular and HSC regeneration after irradiation

Consistent with published data²², we found that irradiation causes an increase in *Vegfc* mRNA expression in the BM. 24 hours after lethal irradiation, an about 100-fold increase of *Vegfc* mRNA was observed in BM non-hematopoietic cells, suggesting that the microenvironment acts as the predominant source of VEGF-C in the post-irradiation marrow (Fig. 4A). VEGF-C protein was also increased in WBM one day after irradiation (Supplementary Figure 6A). Thus, we reasoned that the increase of VEGF-C after irradiation may be important for perivascular niche and hematopoietic recovery.

To evaluate the effect of microenvironment-derived VEGF-C on the hematopoietic niche and HSC regeneration upon injury, we first performed transplantation of WT cells into lethally irradiated $Vc^{i\Delta R26}$ recipient mice. Impaired long-term multilineage reconstitution was observed in $Vc^{i\Delta R26}$ recipients, as evidenced by significantly decreased donor-derived

reconstitution in all peripheral WBC lineages between eight and 16 weeks after transplantation. Donor-derived LKS cells were also reduced in the BM 16 weeks after transplantation (Fig. 4B-D). Decrease of both endomucin+ and LepR+ areas, as well as declined endothelial proliferation, was observed in the irradiated $Vc^{i\Delta R26}$ recipient BM 16 weeks after transplantation (Fig. 4E; Supplementary Figure 6B), indicating that VEGF-C promotes EC proliferation during vascular regeneration. Moreover, some vessels in $Vc^{i\Delta R26}$ recipients lacked basement-membrane laminin coverage. These data indicate that lack of VEGF-C during irradiation-induced injury compromises the recovery of both BM vascular and perivascular components and hematopoietic regeneration.

To evaluate the possibility that the defects attributed to hematopoietic recovery upon loss of niche-derived VEGF-C are caused by impaired homing of HSCs, we labelled WT WBM cells with CFSE and transplanted them into lethally irradiated $Vc^{i\Delta R26}$ or $Vc^{fl/fl}$ mice. We did not find a significant difference in CFSE labelled LKS cells between $Vc^{i\Delta R26}$ or $Vc^{fl/fl}$ recipients 16 hours after transplantation (Supplementary Figure 6C).

To evaluate the effect of niche-derived VEGF-C on HSC self-renewal in the transplantation setting, we employed serial transplantation experiments using $Vc^{i\Delta R26}$ and $Vc^{fl/fl}$ mice as both primary and secondary recipients (Fig. 4F). These experiments demonstrated an impaired multi-lineage reconstitution in $Vc^{i\Delta R26}$ recipients and reduced donor-derived LKS cells 12 weeks after secondary transplantation (Fig. 4G-H). These data suggested that microenvironment-derived VEGF-C is required for HSC self-renewal after transplantation.

To investigate the cellular source of VEGF-C that is required for the niche regeneration after injury, we performed transplantation experiments in $Vc^{\Delta LepR}$ and $Vc^{i\Delta EC}$ mice. An impaired long-term multilineage reconstitution of WT BM cells, reduced LKS numbers and decrease of both LepR⁺ and endomucin⁺ areas was observed in both irradiated $Vc^{\Delta LepR}$ and $Vc^{i\Delta EC}$ recipients (Supplementary Figure 6D-H). In summary, our data suggest that VEGF-C from both ECs and LepR⁺ cells contributes to niche regeneration after irradiation, which in turn affects hematopoietic recovery and HSC self-renewal after transplantation.

Exogenous VEGF-C improves BM recovery after irradiation-induced damage

In light of our findings that niche-derived VEGF-C contributes to niche regeneration and hematopoietic recovery upon transplantation, we investigated whether providing exogenous VEGF-C would have a therapeutic advantage in the recovery from radiation-induced damage. To determine if pre-treatment with VEGF-C can mitigate the effects of irradiation-induced injury in the BM, we injected AAV9 encoding mouse VEGF-C or control protein systemically into WT mice, and sublethally irradiated the mice seven days later using a single 4 Gy dose (Fig. 5A). We confirmed that AAV9 induced an increase in *Vegfc* mRNA in the liver (Supplementary Figure 7A). Seven days after radiation, we observed significantly more ECs and LepR⁺ cells in the irradiated mice that were pre-treated with AAV9 derived VEGF-C than in mice that expressed Fc control or inactivated-VEGF-C (Fig. 5B; Supplementary Figure 7B). Moreover, these mice also showed an increase in BM cellularity and LKS cells (Fig. 5C-D; Supplementary Figure 7C).

To test if administering VEGF-C protein after irradiation has a similar positive effect, we first irradiated mice sublethally with 4 Gy and, 24 hours later, started daily

intraperitoneal injections of 1.25 mg kg^{-1} of VEGF-C for 3 days. We found that the three-day treatment with VEGF-C protein was sufficient to increase the percentage of LKS+ cells in the BM (Supplementary Figure 7D). These data suggested that administering VEGF-C after radiation damage can also improve BM recovery.

Next, we investigated whether administration of VEGF-C would improve hematopoietic recovery upon BM transplantation after lethal irradiation. We injected AAV9 encoding mouse VEGF-C or control protein systemically to WT mice one day after their lethal irradiation using 10 Gy plus BM transplantation (Fig. 5E; Supplementary Figure 7E). We did not observe significant changes in BM cellularity, peripheral WBC cell numbers or spleen size at either two weeks or three weeks after transplantation (Supplementary Figure 7F-G). A transient decrease in the BM B cell percentage and a corresponding transient increase in the myeloid cell percentage was observed at two weeks after transplantation in mice overexpressing VEGF-C (Supplementary Figure 7H). A significant increase of ECs and donor-derived LKS cells was observed both at two and three weeks after transplantation, whereas LepR+ cell numbers were significantly increased by three weeks (Fig. 5F-G). These results suggested that administering VEGF-C after irradiation and transplantation can improve the vascular and perivascular niche recovery as well as hematopoietic regeneration.

VEGF-C promotes EC proliferation and the expression of hematopoietic-regenerative factors after irradiation

To understand the mechanisms how VEGF-C mitigates the radiation-induced damage in the BM niche cells, we isolated BM non-hematopoietic cell fraction from 4 Gy irradiated and non-irradiated $Vc^{fl/fl}$ and $Vc^{\Delta R26}$ mice for scRNA-seq analysis seven days

after irradiation. Graph-based clustering was performed to about 6000 single-cell transcriptomes of the non-hematopoietic niche cells from the BM and the results were visualized using UMAP (Fig. 6A-B; Supplementary Figure 8A-D). We observed three new EC clusters associated with irradiation (damaged ECs, *Aqp1^{hi}* ECs, *Cxcl10* ECs) (Fig. 6B-C). The damaged ECs were characterized by the lack of specific marker transcripts and upregulation of ribosomal gene expression. *Aqp1^{hi}* ECs were characterized by lower expression of SEC-2 markers and higher expression in *Aqp1*, *Ackr1* and *Plvap* (Supplementary Figure 8C). Both damaged ECs and *Aqp1^{hi}* ECs emerged after irradiation, predominantly in irradiated *Vc^{iΔR26}* mice (Fig. 6D). *Cxcl10* ECs were decreased in non-irradiated *Vc^{iΔR26}* mice vs *Vc^{fl/fl}* mice, but increased in irradiated *Vc^{iΔR26}* mice (Fig. 6D). After irradiation, there were more ECs in the S phase, whereas *Vegfc* deletion decreased the proportion of proliferating ECs (Fig. 6D). In agreement with this, we observed a reduction of *Pcna* expression in the irradiated *Vc^{iΔR26}* ECs (Fig. 6E). Notch receptors (*Notch1* and *Notch4*), ligand (*Dll4*) and target gene *Hes1*, which are involved in hematopoietic maintenance and regeneration^{34,43,44}, were decreased in irradiated *Vc^{iΔR26}* EC (Fig. 6E). Many hematopoietic regenerative genes, such as *Angpt2/Tek*, *Sema3f*, and *Thbd*^{6,13,22,44,45} and the VEGF-C receptors (*Flt4* and *Kdr*) were upregulated in irradiated ECs, but not in *Vc^{iΔR26}* ECs in response to irradiation (Fig. 6E). In addition, the irradiation further increased the expression of inflammatory molecules *S100a8* and *S100a9* in *Vc^{iΔR26}* ECs (Fig. 6E).

Interestingly, seven days after irradiation, there were more proliferating LepR+ cells (*Lepr-1*, *Vegfa^{hi}* *Lepr-1* and *Lepr-2* clusters), which were further increased in irradiated *Vc^{iΔR26}* mice (Supplementary Figure 8E). The mesenchymal stem cell gene *Grem1* and known hematopoietic regenerative transcripts, such as *Angpt1*, *Kitl*, *Vcam1* and *Snail2*

^{6,12,46}, were upregulated in LepR+ cells in irradiated $Vc^{fl/fl}$ mice, but not in irradiated $Vc^{i\Delta R26}$ mice (Supplementary Fig. 8F). In contrast, the expression of *S100a8* and *S100a9* was increased significantly in LepR+ cells in irradiated $Vc^{i\Delta R26}$ mice, but not in irradiated $Vc^{fl/fl}$ mice (Supplementary Fig. 8F). Taken together, these results suggest that VEGF-C improves hematopoietic niche recovery after irradiation damage by increasing EC proliferation and by enabling a proper regenerative response in both ECs and LepR cells, as suggested by the induction of hematopoietic regenerative genes and suppression of inflammatory molecules.

Discussion

Our work shows that VEGF-C from BM ECs and LepR+ cells maintains HSC homeostasis by regulating EC-derived signals and LepR+ cells in the perivascular niche. Moreover, we show that VEGF-C can promote vascular and HSC regeneration after myeloablative treatment, implying that VEGF-C contributes to in niche repair after injury (Fig. 7).

Our findings showed that VEGF-C is produced primarily by LepR+ cells and ECs, and that both sources of VEGF-C are functionally required during homeostasis and in response to injury, highlighting the importance of several cell types in co-ordinating the function of the BM hematopoietic niche. The importance of the paracrine cross-talk between the niche cells is emphasized by our finding that although the LepR+ cells do not express the known VEGF-C receptors VEGFR-3 or VEGFR-2, the BM ECs act as cellular intermediates that respond to VEGF-C signalling and consequently promote the maintenance of BM LepR+ cells. When VEGF-C signalling was disrupted, LepR+ cells were unable to sustain proper levels of *Pten*, which is so far the only known factor

associated with LepR⁺ cell maintenance⁴². VEGF-C signalling also sustained the expression of the key niche factor *Cxcl12* (SDF1) in BM ECs. Further studies should identify the specific VEGF-C-induced angiocrine signals from the BM ECs that support the LepR⁺ cells.

In addition to the endothelium, VEGFR-3 and VEGFR-2 are expressed in BM macrophages⁴⁷ and megakaryocytes precursors⁴⁸, which also support HSC maintenance^{49,50}. It is not known if VEGF-C stimulation of these cells influences the hematopoietic niche. Nevertheless, we did not observe significant changes in peripheral blood platelet counts or myeloid cell numbers in the blood or BM, indicating that loss of VEGF-C did not overtly compromise other niche components than ECs and LepR⁺ cells.

Active VEGF-C signalling depends on proteolytic activation of pro-VEGF-C by the complex of pericellular matrix protein CCBE-1 and ADAMTS-3 metalloproteinase^{29,51,52}. Like VEGF-C, both CCBE-1 and ADAMTS-3 are necessary for embryonic erythropoiesis^{53,54}. Our scRNAseq data indicated that BM LepR⁺ cells express *Ccbe1* (data not shown), suggesting its involvement in processing VEGF-C in the adult BM niche.

Our results show that LepR⁺ cells in the adult BM are decreased upon global or EC specific deletion of VEGF-C. Although BM ECs were not significantly affected when *Vegfc* was deleted from adult mice, loss of VEGF-C from LepR⁺ cells during the early post-natal period compromised endothelial proliferation at a time period when the BM vasculature is actively expanding and remodelling. Notably, it has been reported that the *Vc^{fl/fl}* mice show hypomorphic features in the meningeal lymphatic vessels even in the absence of Cre⁵⁵. Nevertheless, we did not observe defects in the adult BM vasculature in these mice.

However, *Vegfc* deletion caused a defective recovery of BM ECs and LepR⁺ cells after irradiation, leading to a compromised hematopoietic regeneration. These results show that genetic deletion of the VEGF-C signalling in actively remodelling vasculature during development or after injury is more harmful than in quiescent adult blood vessels.

Our findings show that VEGF-C contributes to niche regeneration after irradiation. Analysis of EC transcriptional responses to irradiation by RNA-sequencing showed that the hematopoietic regenerative genes, such as *Angpt2/Tek*, *Sema3f*, and *Thbd*, were upregulated after irradiation^{13,22}. Our scRNA-seq analysis also suggested that *Vegfc* deletion suppresses regenerative EC responses to irradiation, including inhibition of cell proliferation, and induction of the inflammatory molecules *S100a8/9*. *Vegfc* deletion also suppressed the expression of hematopoietic regenerative factors (*Angpt1*, *Kitl*, *Vcam1* and *Snail2*) in LepR⁺ cells following irradiation, and induced *S100a8/9*. A previous study has shown that inflammatory signalling from the niche involving *S100a8/9* induces genotoxic stress in HSPCs and influences the progression of bone marrow failure and myelodysplastic syndromes⁵⁶. Furthermore, our data revealed the emergence of damaged ECs and *Aqp1*^{hi} ECs in the BM after irradiation, which was exaggerated upon *Vegfc* loss. These results together highlight the complexity of the responses of BM ECs and LepR⁺ cells to irradiation and the critical function for VEGF-C signalling in promoting the regenerative molecular response.

Our current work extends the function of VEGF-C from fetal erythropoiesis²¹ to adult BM perivascular niche, BM transplantation, and to recovery from irradiation-induced damage. The potential of VEGF-C as a mitigant of irradiation damage in the BM is of

great interest, given its ability to protect two crucial niche components, ECs and LepR+ cells, as well as HSCs, upon radiation-induced injury.

Acknowledgements

We would like to thank Dr. Sinem Karaman for her critical comments; Riitta Kauppinen and Tapio Tainola for expert technical assistance; the Biomedicum Imaging Unit for microscopy support; the Biomedicum FACS core facility for helping with flow cytometry, AAV gene transfer and cell therapy core facility for the service and providing the AAVs, FIMM SCA unit for sc-RNA sequencing and the staff at the Viikki and Biomedicum Helsinki Animal Facilities for excellent animal husbandry. This work was funded by Academy of Finland, iCAN-The Digital Precision Cancer Medicine Platform (grant 320185), the Sigrid Jusélius Foundation (KA), the Cancer Foundation Finland (KA), Hospital District of Helsinki and Uusimaa Research Grant, Helsinki Institute of Life Sciences (HiLIFE), the Magnus Ehrnrooth Foundation (FS) and K. Albin Johanssons Foundation (FS).

Author contributions: F.S, S.C and H.N performed the experiments. V.L, M.J produced and provided VEGF-C protein. L.S. discussed the hypotheses; and contributed to data interpretation and manuscript writing. D.T.S. advised on experimental design and reviewed the manuscript. F.S, H.M and K.A conceived the project, designed experiments, analyzed and interpreted the data, and wrote the manuscript.

Conflicts of Interests: The authors claim no competing interest.

Data and materials availability: Data are available in the GEO database with accession number (GSE128464, GSE144420 and GSE153339). The data that support the findings of this study are available from the corresponding author upon reasonable request.

References:

1. Morrison SJ, Scadden DT. The bone marrow niche for haematopoietic stem cells. *Nature*. 2014;505(7483):327-334.
2. Ramasamy SK, Kusumbe AP, Itkin T, Gur-Cohen S, Lapidot T, Adams RH. Regulation of Hematopoiesis and Osteogenesis by Blood Vessel-Derived Signals. *Annu Rev Cell Dev Biol*. 2016;32:649-675.
3. Gao X, Xu C, Asada N, Frenette PS. The hematopoietic stem cell niche: from embryo to adult. *Development*. 2018;145(2).
4. Bernad A, Kopf M, Kulbacki R, Weich N, Koehler G, Gutierrez-Ramos JC. Interleukin-6 is required in vivo for the regulation of stem cells and committed progenitors of the hematopoietic system. *Immunity*. 1994;1(9):725-731.
5. Sugiyama T, Kohara H, Noda M, Nagasawa T. Maintenance of the hematopoietic stem cell pool by CXCL12-CXCR4 chemokine signaling in bone marrow stromal cell niches. *Immunity*. 2006;25(6):977-988.
6. Ding L, Saunders TL, Enikolopov G, Morrison SJ. Endothelial and perivascular cells maintain haematopoietic stem cells. *Nature*. 2012;481(7382):457-462.
7. Ding L, Morrison SJ. Haematopoietic stem cells and early lymphoid progenitors occupy distinct bone marrow niches. *Nature*. 2013;495(7440):231-235.
8. Greenbaum A, Hsu YM, Day RB, et al. CXCL12 in early mesenchymal progenitors is required for haematopoietic stem-cell maintenance. *Nature*. 2013;495(7440):227-230.
9. Asada N, Kunisaki Y, Pierce H, et al. Differential cytokine contributions of perivascular haematopoietic stem cell niches. *Nat Cell Biol*. 2017;19(3):214-223.
10. Hooper AT, Butler JM, Nolan DJ, et al. Engraftment and reconstitution of hematopoiesis is dependent on VEGFR2-mediated regeneration of sinusoidal endothelial cells. *Cell Stem Cell*. 2009;4(3):263-274.
11. Himburg HA, Muramoto GG, Daher P, et al. Pleiotrophin regulates the expansion and regeneration of hematopoietic stem cells. *Nat Med*. 2010;16(4):475-482.
12. Zhou BO, Ding L, Morrison SJ. Hematopoietic stem and progenitor cells regulate the regeneration of their niche by secreting Angiopoietin-1. *Elife*. 2015;4:e05521.
13. Himburg HA, Sasine J, Yan X, Kan J, Dressman H, Chute JP. A Molecular Profile of the Endothelial Cell Response to Ionizing Radiation. *Radiat Res*. 2016;186(2):141-152.
14. Hassanshahi M, Hassanshahi A, Khabbazi S, Su YW, Xian CJ. Bone marrow sinusoidal endothelium: damage and potential regeneration following cancer radiotherapy or chemotherapy. *Angiogenesis*. 2017;20(4):427-442.
15. Chen Q, Liu Y, Jeong HW, et al. Apelin(+) Endothelial Niche Cells Control Hematopoiesis and Mediate Vascular Regeneration after Myeloablative Injury. *Cell Stem Cell*. 2019.
16. Smith-Berdan S, Nguyen A, Hassanein D, et al. Robo4 cooperates with CXCR4 to specify hematopoietic stem cell localization to bone marrow niches. *Cell Stem Cell*. 2011;8(1):72-83.
17. Winkler IG, Barbier V, Nowlan B, et al. Vascular niche E-selectin regulates hematopoietic stem cell dormancy, self renewal and chemoresistance. *Nat Med*. 2012;18(11):1651-1657.
18. Doan PL, Russell JL, Himburg HA, et al. Tie2(+) bone marrow endothelial cells regulate hematopoietic stem cell regeneration following radiation injury. *Stem Cells*. 2013;31(2):327-337.
19. Himburg HA, Termini CM, Schluskel L, et al. Distinct Bone Marrow Sources of Pleiotrophin Control Hematopoietic Stem Cell Maintenance and Regeneration. *Cell Stem Cell*. 2018;23(3):370-381 e375.

20. Gerber HP, Malik AK, Solar GP, et al. VEGF regulates haematopoietic stem cell survival by an internal autocrine loop mechanism. *Nature*. 2002;417(6892):954-958.
21. Fang S, Nurmi H, Heinolainen K, et al. Critical requirement of VEGF-C in transition to fetal erythropoiesis. *Blood*. 2016;128(5):710-720.
22. Nolan DJ, Ginsberg M, Israely E, et al. Molecular signatures of tissue-specific microvascular endothelial cell heterogeneity in organ maintenance and regeneration. *Dev Cell*. 2013;26(2):204-219.
23. Aspelund A, Tammela T, Antila S, et al. The Schlemm's canal is a VEGF-C/VEGFR-3-responsive lymphatic-like vessel. *J Clin Invest*. 2014;124(9):3975-3986.
24. Ventura A, Kirsch DG, McLaughlin ME, et al. Restoration of p53 function leads to tumour regression in vivo. *Nature*. 2007;445(7128):661-665.
25. Madisen L, Zwingman TA, Sunkin SM, et al. A robust and high-throughput Cre reporting and characterization system for the whole mouse brain. *Nat Neurosci*. 2010;13(1):133-140.
26. Okabe K, Kobayashi S, Yamada T, et al. Neurons limit angiogenesis by titrating VEGF in retina. *Cell*. 2014;159(3):584-596.
27. DeFalco J, Tomishima M, Liu H, et al. Virus-assisted mapping of neural inputs to a feeding center in the hypothalamus. *Science*. 2001;291(5513):2608-2613.
28. Makinen T, Jussila L, Veikkola T, et al. Inhibition of lymphangiogenesis with resulting lymphedema in transgenic mice expressing soluble VEGF receptor-3. *Nat Med*. 2001;7(2):199-205.
29. Jeltsch M, Jha SK, Tvorogov D, et al. CCBE1 enhances lymphangiogenesis via A disintegrin and metalloprotease with thrombospondin motifs-3-mediated vascular endothelial growth factor-C activation. *Circulation*. 2014;129(19):1962-1971.
30. Tammela T, Zarkada G, Wallgard E, et al. Blocking VEGFR-3 suppresses angiogenic sprouting and vascular network formation. *Nature*. 2008;454(7204):656-660.
31. Nurmi H, Saharinen P, Zarkada G, Zheng W, Robciuc MR, Alitalo K. VEGF-C is required for intestinal lymphatic vessel maintenance and lipid absorption. *EMBO Mol Med*. 2015;7(11):1418-1425.
32. Silberstein L, Goncalves KA, Kharchenko PV, et al. Proximity-Based Differential Single-Cell Analysis of the Niche to Identify Stem/Progenitor Cell Regulators. *Cell Stem Cell*. 2016;19(4):530-543.
33. Aran D, Looney AP, Liu L, et al. Reference-based analysis of lung single-cell sequencing reveals a transitional profibrotic macrophage. *Nat Immunol*. 2019;20(2):163-172.
34. Tikhonova AN, Dolgalev I, Hu H, et al. The bone marrow microenvironment at single-cell resolution. *Nature*. 2019;569(7755):222-228.
35. Baryawno N, Przybylski D, Kowalczyk MS, et al. A Cellular Taxonomy of the Bone Marrow Stroma in Homeostasis and Leukemia. *Cell*. 2019;177(7):1915-1932 e1916.
36. Baccin C, Al-Sabah J, Velten L, et al. Combined single-cell and spatial transcriptomics reveal the molecular, cellular and spatial bone marrow niche organization. *Nat Cell Biol*. 2020;22(1):38-48.
37. Butler A, Hoffman P, Smibert P, Papalexi E, Satija R. Integrating single-cell transcriptomic data across different conditions, technologies, and species. *Nat Biotechnol*. 2018;36(5):411-420.
38. Stuart T, Butler A, Hoffman P, et al. Comprehensive Integration of Single-Cell Data. *Cell*. 2019;177(7):1888-1902 e1821.
39. Huang da W, Sherman BT, Lempicki RA. Bioinformatics enrichment tools: paths toward the comprehensive functional analysis of large gene lists. *Nucleic Acids Res*. 2009;37(1):1-13.

40. Huang da W, Sherman BT, Lempicki RA. Systematic and integrative analysis of large gene lists using DAVID bioinformatics resources. *Nat Protoc.* 2009;4(1):44-57.
41. Dieterich LC, Ducoli L, Shin JW, Detmar M. Distinct transcriptional responses of lymphatic endothelial cells to VEGFR-3 and VEGFR-2 stimulation. *Sci Data.* 2017;4:170106.
42. Zhou BO, Yue R, Murphy MM, Peyer JG, Morrison SJ. Leptin-receptor-expressing mesenchymal stromal cells represent the main source of bone formed by adult bone marrow. *Cell Stem Cell.* 2014;15(2):154-168.
43. Poulos MG, Guo P, Kofler NM, et al. Endothelial Jagged-1 is necessary for homeostatic and regenerative hematopoiesis. *Cell Rep.* 2013;4(5):1022-1034.
44. Shao L, Sottoriva K, Palasiewicz K, et al. A Tie2-Notch1 signaling axis regulates regeneration of the endothelial bone marrow niche. *Haematologica.* 2019;104(11):2164-2177.
45. Xu C, Gao X, Wei Q, et al. Stem cell factor is selectively secreted by arterial endothelial cells in bone marrow. *Nat Commun.* 2018;9(1):2449.
46. Wei Q, Nakahara F, Asada N, et al. Snai2 Maintains Bone Marrow Niche Cells by Repressing Osteopontin Expression. *Dev Cell.* 2020.
47. Zhang Y, Lu Y, Ma L, et al. Activation of vascular endothelial growth factor receptor-3 in macrophages restrains TLR4-NF-kappaB signaling and protects against endotoxin shock. *Immunity.* 2014;40(4):501-514.
48. Thiele W, Krishnan J, Rothley M, et al. VEGFR-3 is expressed on megakaryocyte precursors in the murine bone marrow and plays a regulatory role in megakaryopoiesis. *Blood.* 2012;120(9):1899-1907.
49. Bruns I, Lucas D, Pinho S, et al. Megakaryocytes regulate hematopoietic stem cell quiescence through CXCL4 secretion. *Nat Med.* 2014;20(11):1315-1320.
50. Winkler IG, Sims NA, Pettit AR, et al. Bone marrow macrophages maintain hematopoietic stem cell (HSC) niches and their depletion mobilizes HSCs. *Blood.* 2010;116(23):4815-4828.
51. Joukov V, Sorsa T, Kumar V, et al. Proteolytic processing regulates receptor specificity and activity of VEGF-C. *EMBO J.* 1997;16(13):3898-3911.
52. Xu Y, Yuan L, Mak J, et al. Neuropilin-2 mediates VEGF-C-induced lymphatic sprouting together with VEGFR3. *J Cell Biol.* 2010;188(1):115-130.
53. Zou Z, Enis DR, Bui H, et al. The secreted lymphangiogenic factor CCBE1 is essential for fetal liver erythropoiesis. *Blood.* 2013;121(16):3228-3236.
54. Janssen L, Dupont L, Bekhouche M, et al. ADAMTS3 activity is mandatory for embryonic lymphangiogenesis and regulates placental angiogenesis. *Angiogenesis.* 2016;19(1):53-65.
55. Antila S, Karaman S, Nurmi H, et al. Development and plasticity of meningeal lymphatic vessels. *J Exp Med.* 2017;214(12):3645-3667.
56. Zambetti NA, Ping Z, Chen S, et al. Mesenchymal Inflammation Drives Genotoxic Stress in Hematopoietic Stem Cells and Predicts Disease Evolution in Human Pre-leukemia. *Cell Stem Cell.* 2016;19(5):613-627.

Figure Legends

Figure 1. *VEGF-C regulates the integrity of the BM LepR+ HSC niche.*

A, Relative *Vegfc* mRNA level in sorted WT PECAM1+ ECs and LepR+ stromal cells by q-PCR (normalized to WBM; n=2 individual mice per group). **B**, Experimental outline of sc-RNA seq analysis of LepR+ cells and VE-Cadherin+ ECs from *Lepr-Cre;tdTomato* BM. **C**, UMAP plots of BM LepR-tdTomato+ cells and VE-Cadherin+ ECs (left). Feature plot showing *Lepr*, *Cdh5* (right). **D**, Feature plot showing *Vegfc*, *Flt4* and *Kdr* expression. **E**, Experimental setup for evaluating the effects of *Vegfc* deletion in the BM. *Vegfc* was deleted from adult BM by giving five tamoxifen injections to 7-10 weeks old *Rosa26-CreER^{T2};Vegfc^{fllox/fllox}* mice. **F**, Representative confocal immunofluorescence images of femur sections from *Vc^{iΔR26}* and *Vc^{fl/fl}* mice five months after deletion stained for ECs (endomucin, green) and perivascular cells (LepR, red). Quantifications are shown on the right (n=5-6 individual mice per group). Scale, 50μm. **G**, Quantification of HSPC subsets per femur from seven month old *Vc^{iΔR26}* mice and *Vc^{fl/fl}* littermate controls using CD48 and CD150 staining (n=13-14 individual mice per group). Quantification of HSPC subsets per femur from 22-23 month old *Vc^{iΔR26}* mice and *Vc^{fl/fl}* littermate controls (n=6 individual male mice per group). Reported values are mean ± SD. Statistical significance was determined using Student's t-test (two tailed, unpaired).

Figure 2. *Endothelial cells serve as a functionally significant source of VEGF-C in the BM.*

A, Experimental setup for evaluating the effects *Vegfc* deletion in ECs. *Vegfc* was deleted from ECs in 7-10 weeks old *Cdh5-CreER^{T2};Vegfc^{fllox/fllox}* mice using tamoxifen injections. **B**, Representative confocal immunofluorescence images of femur sections from *Vc^{iΔEC}* mice and their littermate controls stained for ECs (endomucin, green) and LepR+ perivascular

cells (red). Quantification is shown on the right (n=6 individual mice per group). Scale, 50µm. **C**, Quantification of HSPC subsets per femur from $Vc^{fl/fl}$ and $Vc^{i\Delta EC}$ mice (n=13-14 individual mice) using CD48 and CD150 staining. **D**, Experimental outline for sc-RNA seq analysis of LepR+ cells and VE-Cadherin+ ECs from WT, $Vc^{fl/fl}$ and $Vc^{i\Delta EC}$ mice. **E**, UMAP plot of integrated BM ECs and LepR+ cells isolated from WT, $Vc^{fl/fl}$ and $Vc^{i\Delta EC}$ mice (left). UMAP plots showing the clustering of integrated BM ECs and LepR+ cells from WT, $Vc^{fl/fl}$ and $Vc^{i\Delta EC}$ mice (right). **F**, Dotplot showing selected differentially expression genes in SECs (SEC-1 and SEC-2) and AECs (Arteriolar ECs and Arterial ECs) after endothelial *Vegfc* deletion in comparison with $Vc^{fl/fl}$ mice. **G**, Relative *Cxcl12* mRNA levels in isolated BM ECs from $Vc^{i\Delta EC}$ and littermate control mice analysed by q-PCR. **H**, Comparison of relative cell counts in Lepr-1,-2,-3,-4,-5 clusters from $Vc^{fl/fl}$ and $Vc^{i\Delta EC}$ mice. **I**, Dotplot showing selected differentially expression genes in LepR+ cells (Lepr-1, Lepr-2, Lepr-3) after endothelial *Vegfc* deletion in comparison with $Vc^{fl/fl}$ mice. **J**, Relative *Pten* mRNA levels in isolated BM LepR+ cells from $Vc^{i\Delta EC}$ and littermate control mice analysed by q-PCR.

Figure 3. *LepR+* cell derived VEGF-C contributes to maintenance of functional HSCs in the BM.

A, Experimental setup for evaluating the effects of LepR+ cells derived VEGF-C. *Vegfc* was deleted from LepR+ cells using *Lepr-Cre*. BM of 7-10 weeks old mice was analysed for niche cell and HSC phenotypes. WBM from 10 weeks old $Vc^{\Delta Lepr}$ or $Vc^{fl/fl}$ mice was transplanted competitively with CD45.1 WBM to lethally irradiated CD45.1 mice. **B**, Representative confocal immunofluorescence images of femur sections from $Vc^{\Delta Lepr}$ and $Vc^{fl/fl}$ littermate controls stained for ECs (endomucin, green) and LepR+ perivascular cells (red), and graphs showing quantification (n=6-7 individual mice per group). Scale, 50µm.

C, Quantification of HSPC subsets per femur from $Vc^{\Delta Lepr}$ and $Vc^{fl/fl}$ littermate control mice (n=4 individual mice per group) using CD48 and CD150 staining. **D**, Competitive transplantation of WBM from $Vc^{\Delta Lepr}$ and their $Vc^{fl/fl}$ littermate control mice into lethally irradiated WT CD45.1 recipients (2 independent transplants with 3-4 recipients per condition per transplant). Shown is multi-lineage donor chimerism from peripheral blood at the indicated timepoints after competitive transplantation. **E**, Quantification of LKS cells derived from $Vc^{\Delta Lepr}$ or $Vc^{fl/fl}$ mice in the BM 16 weeks after transplantation. Reported values are mean \pm SD. Statistical significance was determined using Student's t-test (two tailed, unpaired).

Figure 4. Loss of VEGF-C from the BM microenvironment delays vascular and HSC regeneration after irradiation

A, Experimental setup for evaluating *Vegfc* expression level in the BM after irradiation using q-PCR. Relative *Vegfc* mRNA level in WBM, in sorted CD45⁻Ter119⁻ stromal cells and CD45⁺Ter119⁺ hematopoietic cells 24 h after 10 Gy radiation (normalized to untreated WBM; n=2 individual mice). **B**, Experimental setup for evaluating the efficiency of engraftment of WT WBM in lethally irradiated $Vc^{i\Delta R26}$ and $Vc^{fl/fl}$ mice. **C**, Transplantation of WT WBM (CD45.1) into lethally irradiated $Vc^{i\Delta R26}$ mice and their $Vc^{fl/fl}$ littermate hosts. Representative flow graph in the total WBC from peripheral blood 12 weeks after transplantation is shown (left). The kinetics of multi-lineage donor chimerism from peripheral blood after transplantation is shown (right, n=6-8 individual mice per group). **D**, Quantification of BM LKS numbers in lethally irradiated $Vc^{i\Delta R26}$ mice and their $Vc^{fl/fl}$ littermate recipients 16 weeks after transplantation (n=6-8 individual mice per group). **E**, Representative confocal immunofluorescence images and quantification (n=4-5 individual mice per group) of femur sections from from $Vc^{i\Delta R26}$ mice and their littermate controls

stained for ECs and basement membranes (endomucin, green; Laminin, white) and LepR cells (red). Scale, 50 μ m. **F**, Experimental setup for serial transplantation. WBM (CD45.1) from lethally irradiated primary $Vc^{i\Delta R26}$ and $Vc^{fl/fl}$ recipients was transplanted competitively with CD45.2 WBM into lethally irradiated secondary $Vc^{i\Delta R26}$ and $Vc^{fl/fl}$ recipients. **G**, Multi-lineage donor chimerism from peripheral blood after secondary competitive transplantation (2 independent transplants with 3 recipients per condition per transplant). **H**, Quantification of BM LKS numbers in secondary $Vc^{i\Delta R26}$ mice and their $Vc^{fl/fl}$ littermate controls 16 weeks after transplantation. Reported values are mean \pm SD. Statistical significance was determined using Student's t-tests (two tailed, unpaired).

Figure 5. VEGF-C improves BM recovery after irradiation-induced damage.

A, Experimental setup for evaluating the effects of exogenous VEGF-C upon irradiation induced injury. Adeno-associated viral vector encoding mouse VEGF-C or control protein was injected systemically to WT mice seven days before irradiation. BM was analyzed seven days after irradiation. **B**, Quantification of BM VE-cad⁺ ECs and LepR⁺ cells in VEGF-C treated WT mice seven days after 4 Gy irradiation by flow cytometry (n=6-8 individual mice per group). **C**, Quantification of LKS cells per femur (n=6-8 individual mice per group) by flow cytometry. **D**, H&E staining of femur sections seven days after 4 Gy irradiation (n=6-8 individual mice per group). Scale, 50 μ m. **E**, Experimental setup for evaluating the effects of exogenous VEGF-C on the efficiency of hematopoietic engraftment after transplantation. Adeno-associated viral vector encoding mouse VEGF-C or control protein was injected systemically to WT mice one day after lethal irradiation and BM transplantation. BM was analyzed two and three weeks after transplantation. **F-G**, Flow cytometry quantification of BM ECs, LepR⁺ cells and LKS cells in mice treated with VEGF-C after lethal irradiation and BM transplantation (n=3 per group per time-point).

Reported values represent the mean \pm SD. Statistical significance was determined using Student's t-test or one-way ANOVA multiple comparisons test.

Figure 6. VEGF-C promotes BM EC proliferation and increases the expression of hematopoietic-regenerative factors after irradiation. **A**, Experimental setup for evaluating the effects of *Vegfc* in the BM upon irradiation. *Vegfc* was deleted from the BM in 10 weeks old *Rosa26-CreER^{T2};Vegfc^{flox/flox}* mice using tamoxifen injections. *Vc^{iΔR26}* and *Vc^{fl/fl}* Mice received 4Gy irradiation after two-week tamoxifen washout. Niche cells were isolated from irradiated (IR) *Vc^{iΔR26}* and *Vc^{fl/fl}* mice and their non-irradiated (N-IR) controls seven days after irradiation and analysed using scRNA-seq. **B-C**, UMAP plot showing the clustering from integrated non-hematopoietic BM stroma cells from irradiated (IR) *Vc^{iΔR26}* and *Vc^{fl/fl}* mice and their non-irradiated (N-IR) controls. UMAP plot showing non-hematopoietic BM stroma cells from irradiated *Vc^{iΔR26}* and *Vc^{fl/fl}* mice and their non-irradiated controls separately. Note that damaged ECs (green arrowhead) and *Aqp1^{hi}* ECs (blue arrowhead) are increased after irradiation. **D**, Percentages of the clusters (damaged ECs, *Aqp1^{hi}* ECs, *Cxcl10* ECs) and quantification of ECs in S phase. **E**, Dotplot showing selected differentially expressed genes in SECs (SEC-1, SEC-2, *Cxcl10* ECs), damaged ECs, *Aqp1^{hi}* ECs and AECs. Analysis of differentially expressed genes was performed between IR;*Vc^{fl/fl}* vs N-IR;*Vc^{fl/fl}* and IR;*Vc^{iΔR26}* vs N-IR;*Vc^{iΔR26}*.

Figure 7. VEGF-C contributes to BM niche maintenance and regeneration after irradiation. Schematic models describing the BM microenvironment with ECs, LepR+ cells, HSCs and VEGF-C. **(I)** During homeostasis, HSCs reside in and are maintained by the intact perivascular niche composed of ECs and LepR+ cells. VEGF-C from both LepR+ cells and ECs maintains an intact BM perivascular niche that is required for HSC

maintenance. When *Vegfc* is deleted from ECs or LepR cells, genes related to interferon response are upregulated, and *Cxcl12* and *Pten* are decreased in BM ECs and LepR+ cells, respectively, which leads to niche impairment and compromised HSC maintenance.

II). (a) After irradiation and HSC transplantation, *Vegfc* expression in the niche is upregulated. Microenvironment-derived VEGF-C contributes to endothelial and LepR+ cell regeneration, which in turn is essential for HSC regeneration. **(b)** When *Vegfc* is deleted from the BM microenvironment, genes related to inflammation are upregulated and the proliferation of ECs is decreased, which leads to impaired niche regeneration. Niche-derived hematopoietic regenerative factors are also decreased, resulting in a decreased recovery of HSCs. **(c)** Overexpression of VEGF-C improves vascular regeneration, which leads to a better hematopoietic recovery after irradiation or transplantation.

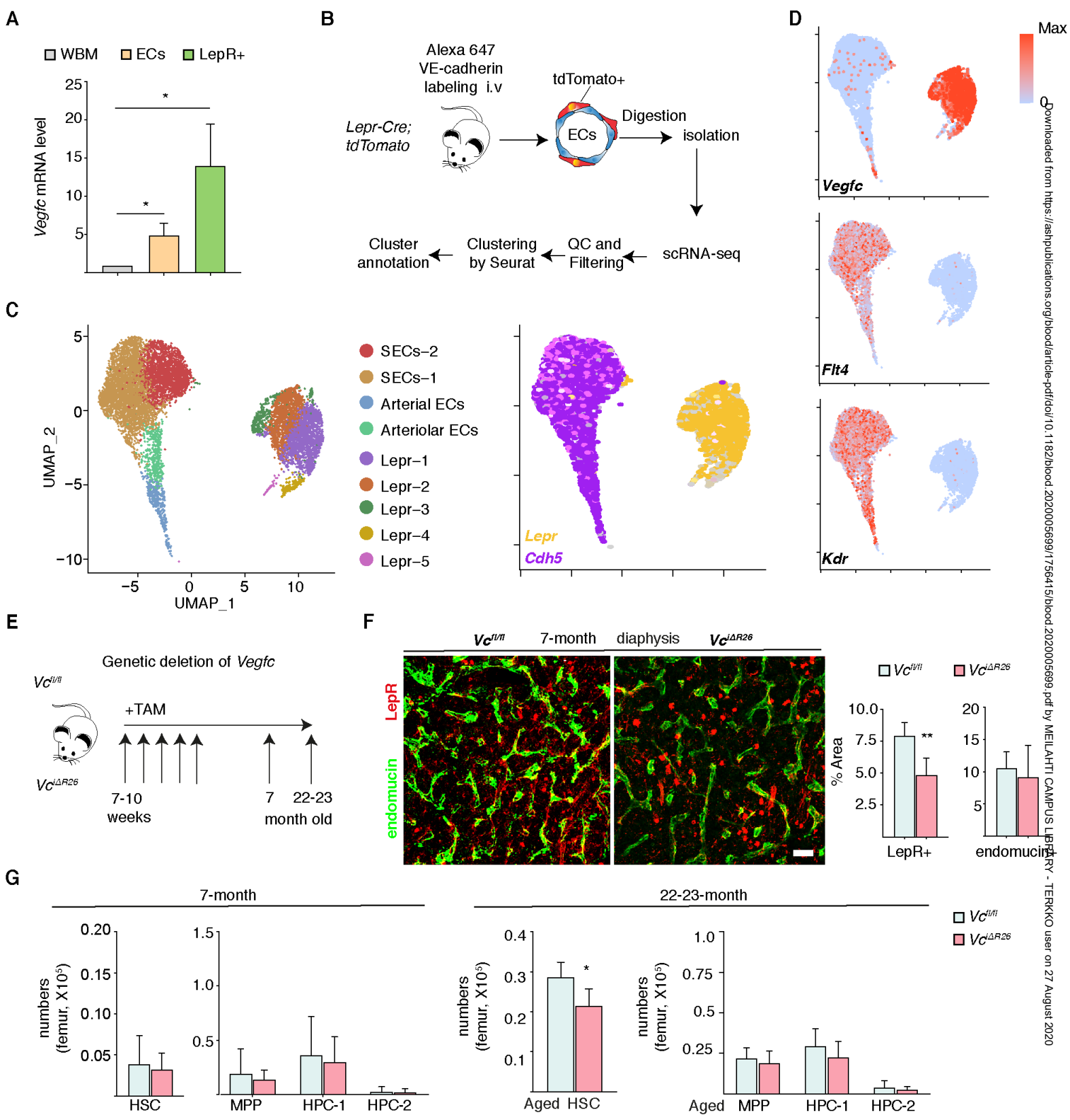


Fig. 1

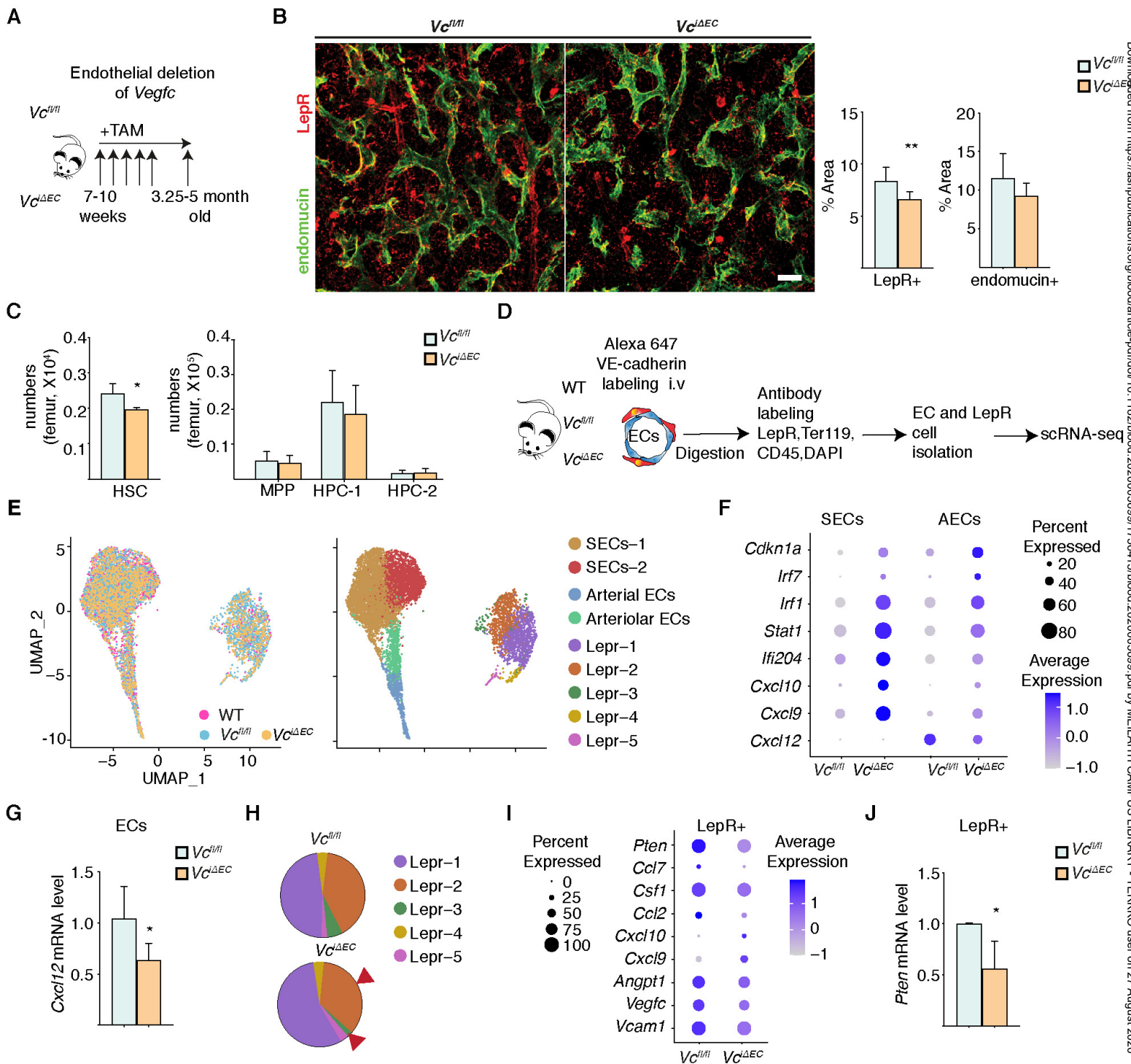


Fig. 2

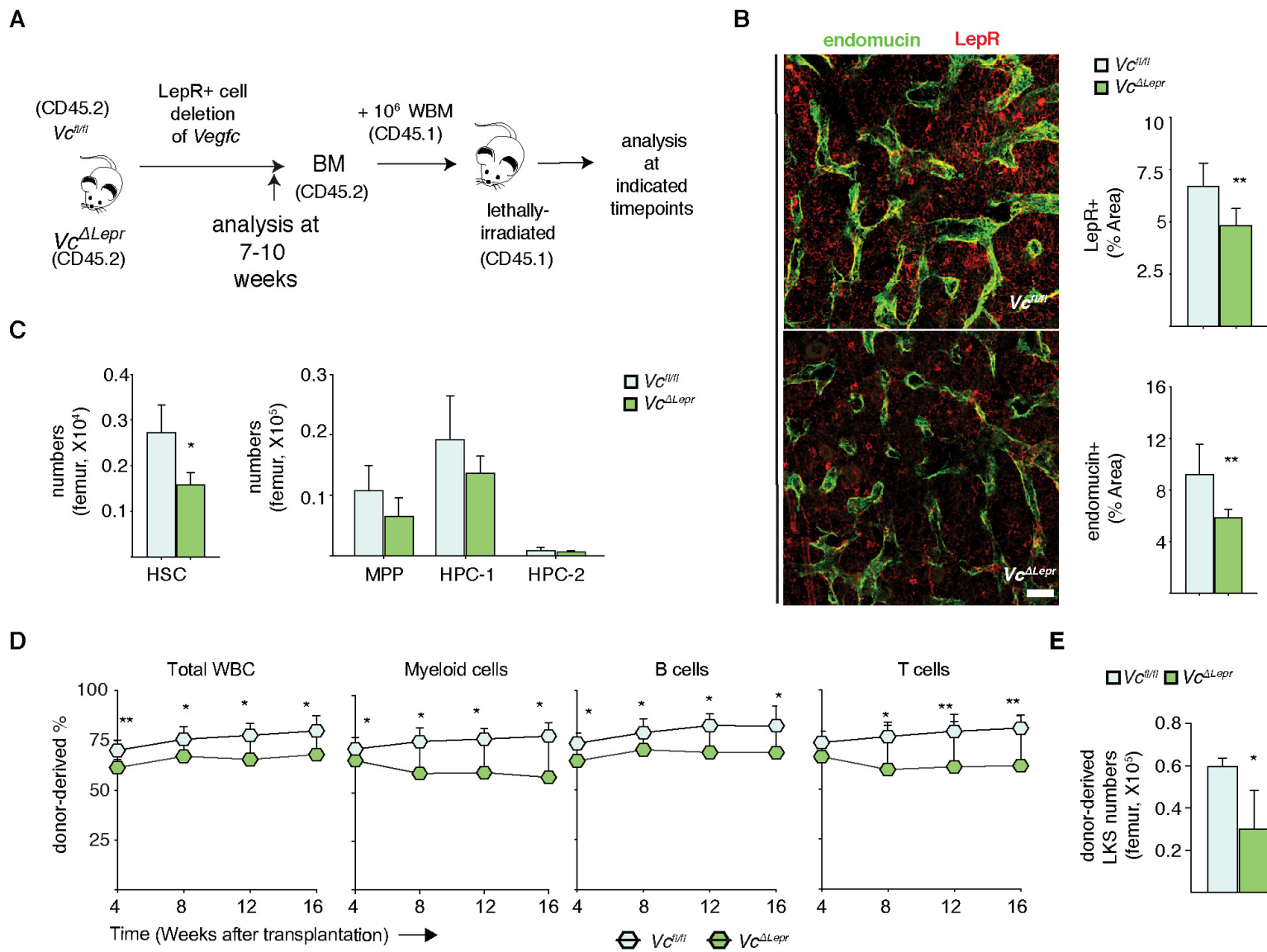


Fig. 3

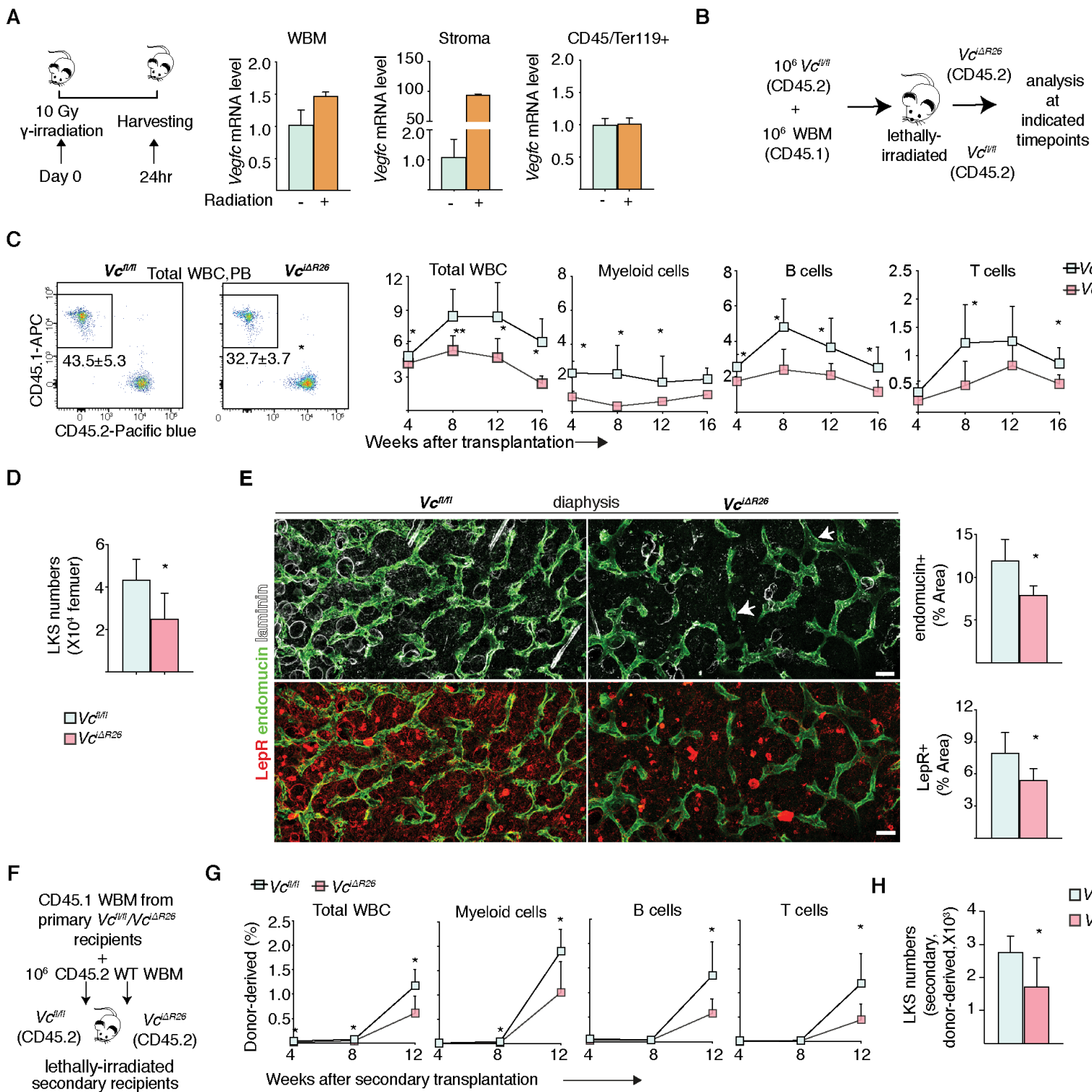


Fig. 4

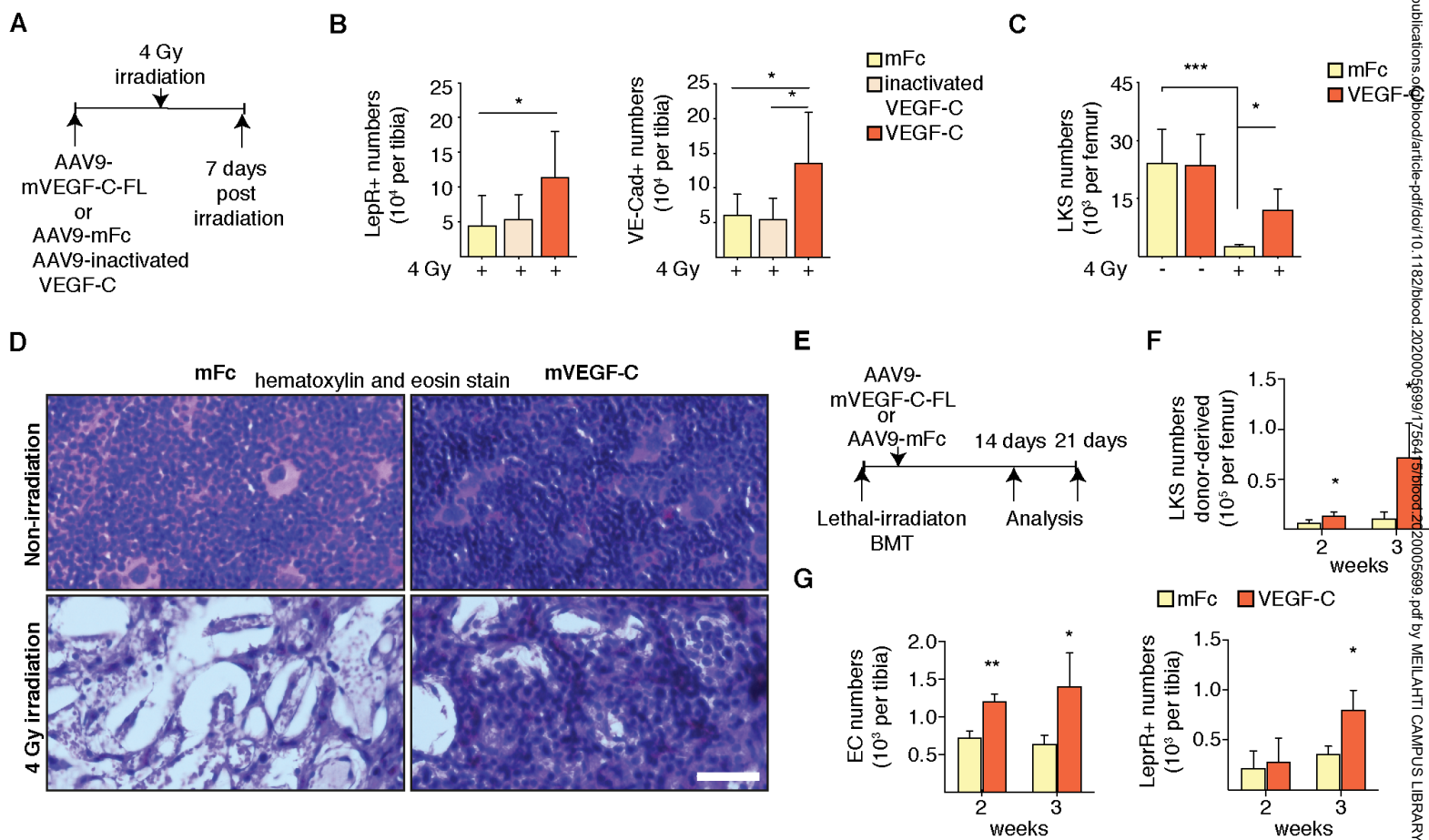


Fig 5

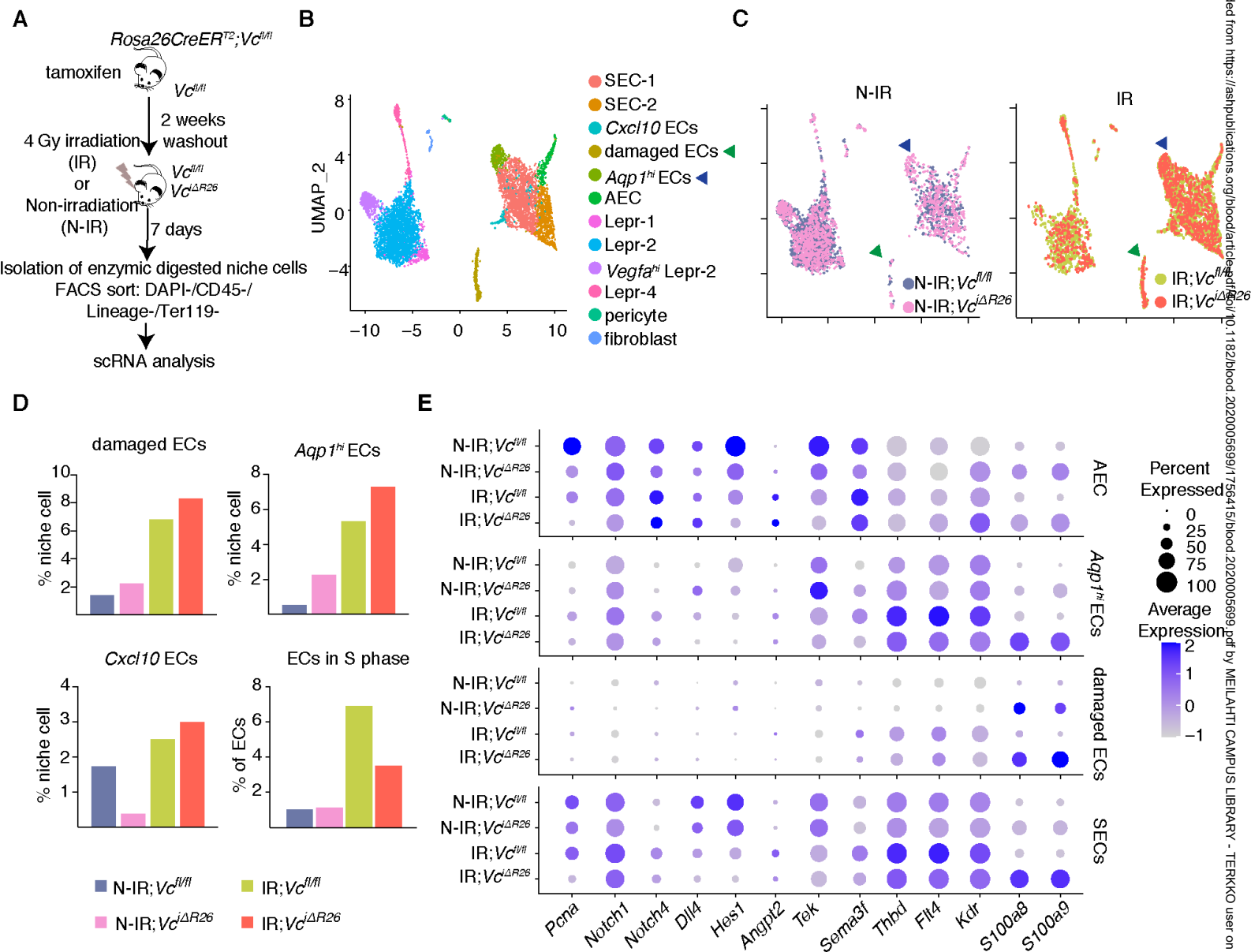


Fig. 5

A

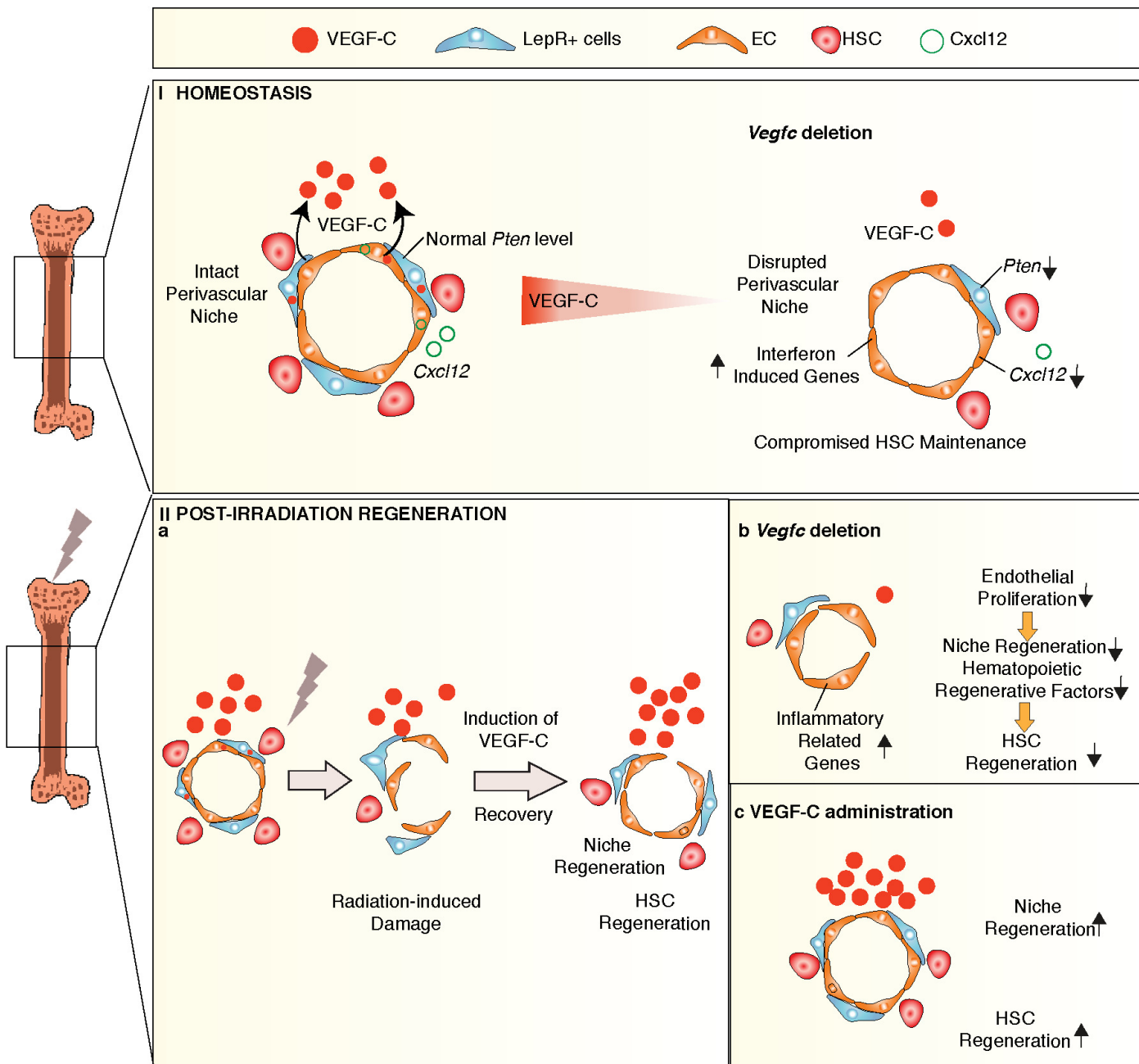


Fig7